Original Article

Transthyretin-induced increase in circ_0007411 represses neovascularization of human retinal microvascular endothelial cells in hyperglycemia via the miR-548m/PTPN12/SKP1/EGFR pathway

Di Hu[1], Yikun Tian[1], Lu Ye[1], Yu Xin[1]^, Jun Shao[2]^

[1]The Key Laboratory of Industrial Biotechnology, Ministry of Education, National Engineering Research Center for Cereal Fermentation and Food Biomanufacturing, Jiangnan University, Wuxi, China; [2]Department of Ophthalmology, The Affiliated Wuxi People's Hospital of Nanjing Medical University, Wuxi, China

Contributions: (I) Conception and design: Y Xin, J Shao; (II) Administrative support: Y Xin, J Shao; (III) Provision of study materials or patients: D Hu, Y Tian, L Ye; (IV) Collection and assembly of data: D Hu, Y Tian, L Ye; (V) Data analysis and interpretation: D Hu, Y Tian, L Ye; (VI) Manuscript writing: All authors; (VII) Final approval of manuscript: All authors.

Correspondence to: Yu Xin. The Key Laboratory of Industrial Biotechnology, Ministry of Education, National Engineering Research Center for Cereal Fermentation and Food Biomanufacturing, Jiangnan University, Wuxi 214122, China. Email: yuxin@jiangnan.edu.cn; Jun Shao. Department of Ophthalmology, The Affiliated Wuxi People's Hospital of Nanjing Medical University, Qing Yang Road 299, Wuxi 214023, China. Email: shaojun1983@hotmail.com.

Background: To investigate the mechanism of transthyretin (TTR) induced high expression of circ_0007411 and its parent gene, protein tyrosine phosphatase nonreceptor type 12 (*PTPN12*) in human retinal microvascular endothelial cells (hRECs) cultivated under high glucose condition.

Methods: The levels of *PTPN12*, circ_0007411, miR-548m, S-phase kinase associated protein 1 (*SKP1*) and epidermal growth factor receptor (*EGFR*) were detected by quantitative reverse transcription-polymerase chain reaction (qRT-PCR). The direct interaction between circ_0007411/*PTPN12* and miR-548m was investigated via Dual-luciferase reporter assay. The physiological characterization of hRECs was investigated through Cell Counting Kit-8 (CCK-8), 5-Ethynyl-2'-deoxyuridine (EdU) labelling, Transwell, flow cytometry (FCM), wound healing, and tube formation assays. Co-immunoprecipitation (Co-IP) was used to detect the interaction between PTPN12 and SKP1. The function of PTPN12 against diabetic retinopathy (DR) was studied in streptozotocin (STZ) induced DR C57BL/6 mice.

Results: The levels of circ_0007411 was increased in hRECs in hyperglycemia with the induction of TTR. The overexpressed circ_0007411 could significantly enhance the level of *PTPN12* and repress that of miR-548m, and it could enhance apoptosis and prohibit the proliferation, migration, and tube formation of hRECs. miR-548m mimics enhanced the proliferation, migration, and tube formation of hRECs by reducing the expression level of *PTPN12* and promoting that of *EGFR*, whereas circ_0007411 rescued it. The direct binding of *PTPN12* and *SKP1* was confirmed by Co-IP. Additionally, the anti-neovascularization function of *PTPN12* was confirmed in a STZ-induced mouse model of DR.

Conclusions: In hyperglycemia, the TTR-induced increase in circ_0007411 could repress retinal neovascularization via the miR-548m/PTPN12/SKP1/EGFR pathway.

Keywords: Circ_0007411; protein tyrosine phosphatase nonreceptor type 12 (PTPN12); miR-548m; S-phase kinase associated protein 1 (SKP1); anti-neovascularization

^ ORCID: Yu Xin, 0000-0002-5396-4319; Jun Shao, 0000-0003-3477-4568.

Submitted Feb 22, 2022. Accepted for publication Apr 27, 2022. This article was updated on August 07, 2024.
The original version is available at: http://dx.doi.org/10.21037/atm-22-1276
doi: 10.21037/atm-22-1276

Introduction

In response to the dramatically increasing prevalence of diabetes (1), diabetic retinopathy (DR) has been identified as a major cause of blindness and visual impairment (2,3). During diabetes, the sustained hyperglycemia and the subsequent ischemic retinal hypoxia have been considered as the important triggers for vascular dysfunction; and the downstream switches, such as the hypoxia-inducible factor-1α (HIF-1α) or vascular endothelial growth factor (VEGF) associated pathways, would be stimulated to promote the progression of DR, bringing with the clinical properties of DR, including microaneurysms, hemorrhages, lipid exudates, diabetic macular edema (DME), retinal capillary occlusion, cotton-wool spots, and neovascularization (NV) (3,4). In addition, as recently reported, inflammation associated pathways have also been considered as the key factors in the progression of DR, including nuclear factor-κB (NF-κB), Toll-like receptor (TLR) and Jak/Stat pathways; and the chronic low-grade inflammation in retina could promote the edema and NV in DR (5).

The prevention of retinal NV has recently been considered as the basic principle for the clinical therapy of DR, and to rescue retinal vascular leakage and angiogenesis in DR, anti-VEGF antibodies, including pegaptanib, ranibizumab, and bevacizumab, have been applied through intraocular injection (6). However, the development of more efficient therapy protocols requires systematic investigation into the mechanism of retinal microvascularization.

Circular RNAs (circRNAs) are the back-splicing products after transcription, without 5'–3' polarity and poly A tails, circRNAs are more stable than mRNAs, and they have been proved as sponges of micro-RNAs, or to interact with RNA binding proteins, regulate mRNAs stability, modulate gene transcription and translate proteins (7). And recently, circRNAs have emerged as a hot topic in the study of various diseases, including diabetes and eye disease (8,9), some of them have been demonstrated to play vital roles in the procession of DR by regulating the angiogenesis, proliferation, apoptosis, and inflammatory response in the retina of DR patients and animal models (10). In addition, some circRNAs have been reported to affect the physiological properties of retinal microvascular endothelial cells, including circRNA-FoxO1 (11), circHIPK3 (12), and circCOL1A2 (13). These studies suggest circRNAs may be potential biomarkers for the diagnosis of DR or molecular targets clinical therapy.

Protein tyrosine phosphatase nonreceptor type 12 (*PTPN12*) is located at chromosome 7q11.23 (14) and belongs to the protein tyrosine phosphatase family. *PTPN12* has been reported to participate in tumor occurrence and development (15), embryonic development, cell apoptosis, cell cycle, and metabolism (16), and has also been reported to exert antitumor function by regulating epidermal growth factor receptor (EGFR) (17). Circ_0007411 is one circRNA form of *PTPN12*, but its role in the mechanism of NV has rarely been investigated.

In our previous work, transthyretin (TTR) was shown to have an anti-angiogenic function in DR, mediated through the PABPC1/lncRNA MEG3/miR-223-3p/FBXW7 and hnRNPA2B1/STAT4/miR-223-3p/FBXW7 signaling axes (18-20). However, it is not known if TTR can affect or regulate circRNAs. In this study, after human retinal endothelial cells (hRECs) was treated with TTR, abnormally expressed circRNAs were screened via RNA sequencing (RNA-Seq), and circ_0007411 was significantly promoted in hyperglycemia with exogenous TTR. Circ_0007411 has not been reported as associated with the progression of DR; in addition, bioinformatics assay indicated that circ_0007411 contained the same target sites of miR-548m in the 3'-untranslated region (UTR) of *PTPN12* mRNA. The relationship between circ_0007411, *PTPN12*, and miR-548m was investigated in hRECs, and the anti-NV function of *PTPN12* was investigated in a STZ-induced model of DR in C57BL/6 mice. The mechanisms were also studied. We present the following article in accordance with the ARRIVE reporting checklist (available at https://atm.amegroups.com/article/view/10.21037/atm-22-1276/rc).

Methods

Cell culture and reagents

hRECs were obtained from the Cell Bank of the Chinese Academy of Science (Shanghai, China), using high-glucose DMEM (Gibco, USA) containing 10% FBS for cultivation, as described in our previous work (15-17). Anti-PTPN12, -SKP1, -EGFR, and -glyceraldehyde 3-phosphate dehydrogenase (GAPDH) antibodies were

Table 1 Primers for qRT-PCR assay

Target gene	Primers
circ_0007411	F: 5'-GCCAGACCATGATGTTCCTTC-3'
	R: 5'-TGCTAAAGGTCCTTGAGTTGC-3'
PTPN12	F: 5'-CTCCTCCCCTACCTGAAAG-3'
	R: 5'-TTCACTTGCTAACACAAACGA-3'
SKP1	F: 5'-GACCATGTTGGAAGATTTGGGA-3'
	R: 5'-TGCACCACTGAATGACCTTTT-3'
EGFR	F: 5'-CTACAACCCCACCACGTACC-3'
	R: 5'-CGCACTTCTTACACTTGCGG-3'
miR-548m	F: 5'-AAGCGACCCAAAGGTATTTGT-3'
	R: 5'-GTCGTATCCAGTGCAGGGT-3'
cel-miR-39-3p	F: 5'-GTCACCGGGTGTAAATCAG-3'
	R: 5'-GGTCCAGTTTTTTTTTTTTTTCAAG-3'
GAPDH	F: 5'-GCACCGTCAAGGCTGAGAAC-3'
	R: 5'-TGGTGAAGACGCCAGTGGA-3'

qRT-PCR, quantitative real-time polymerase chain reaction; PTPN12, protein tyrosine phosphatase nonreceptor type 12; SKP1, S-phase kinase associated protein 1; EGFR, epidermal growth factor receptor; GAPDH, glyceraldehyde 3-phosphate dehydrogenase.

purchased from Cell Signaling Technology (Beverly, MA, USA), while the quantitative real-time polymerase chain reaction (qRT-PCR) primers for circ_0007411, *PTPN12*, miR-548m, cel-miR-39-3p, and GAPDH were synthesized by GenePharma (Suzhou, China). The mouse *PTPN12* overexpression adeno-associated virus (AAV), shPTPN12 (5'-GGACATACTGCCATTTGATCACGA ATGATCAAATGGCAGTATGTCC-3'), circ_0007411 overexpression plasmid (OECIRC), si-circ_0007411-1 (5'-GUAUUCAUUGCAGUUGAUCTT-3'), si-circ_0007411-2 (5'-CAUUGCAGUUGAUCACAGCTT-3'), and the miR-548m mimic and inhibitor were synthesized by GenePharma (Suzhou, China). The cells were grouped as high glucose (HG), overexpression-negative control (OE-NC), OE-7411, si-NC, si-7411-1, si-7411-2, mimic-NC, miR-548m mimic, mimic + 7411, inhibitor NC, and miR-548m inhibitor; and each experiment was repeated for at least three times.

RNA-Seq

Trizol was used to extract total RNA from hRECs cultivated in a high-glucose environment with or without 4 μmol/L TTR in accordance with the manufacturer's handbook (Takara, Dalian, China). After the RNA concentration was detected with a Qubit RNA detection kit (Invitrogen, Carlsbad, CA, USA), the extracted RNA was subjected to sequencing, and the raw data were deposited in the Gene Expression Omnibus-National Center for Biological Information (GEO-NCBI; GSE117238) (21). After screening using FastQC (V0.11.9) and NGSQC software (V2.3.3) (22), circRNAs were further identified by Tophat2 (v2.1.1), Find_circ (v1.2), and CIRCexplorer2 software (23), and differentially expressed circRNAs were identified using the Limma (v3.44.3) software package (24).

Cell migration and healing

As described in our previous work (18-20), hRECs were inoculated in the Transwell insert, incubated for 30 h, fixed with 4% paraformaldehyde, stained with crystal violet, and counted under light microscope. Using a wound healing assay kit (ab242285), the hRECs were plated in six-well culture dishes and grown to confluence. A defined gap was then created by the insert of the kit, and wound healing was monitored over 24 h. The relative wound density (RWD) was detected and calculated using an Olympus IX-73 microscope.

Tube formation

After a 0.5 h incubation at 37 ℃ in in a 48-well plate, the hRECs were inoculated into the basement membrane matrix (BD Biosciences) for a further 3 h incubation at 37 ℃, and the tube formation process was observed and monitored using an Olympus IX-73 microscope (18-20).

qRT-PCR

As described in our previous work (18-20), after extraction of the total RNAs and total miRNAs, the expression of *PTPN12* mRNA and circ_0007411 in hRECs was detected using Moloney murine leukemia virus (M-MLV) reverse transcriptase and a SYBR Green Real-Time PCR Master Mix (Invitrogen, Carlsbad, CA, USA), with GAPDH was as the internal control. The level of miR-548M was detected using the mirVana^{TM} qRT-PCR miRNA detection kit (Invitrogen, Carlsbad, CA, USA), with cel-miR-39-3p spike-in as the internal control. The primers are listed in *Table 1*.

Flow cytometry (FCM)

Apoptotic cells were labelled using the Annexin V/FITC kit (BD Biosciences, San Jose, CA, USA) in accordance with the manufacturer's instructions, and monitored by FCM.

Cell Counting Kit-8 (CCK-8) assay

The proliferation of hRECs was investigated using a CCK-8 kit (Dojindo Laboratories, Kumamoto, Japan) as described in our previous work (18,21).

5-Ethynyl-2'-deoxyuridine (EdU)

The EdU assay was conducted in accordance with the manufacturer's handbook (RiboBio, Guangzhou, China). After hRECs were seeded in a 48-well plate, 50 μM EdU was added to each well, and the plate was incubated at 37 ℃ for 4 h. The cells were fixed in 4% paraformaldehyde and permeabilized by 0.5% Triton X-100 then sequentially treated with Apollo 488 fluorescent dye solution and 4',6-diamidino-2-phenylindole (DAPI) solution. The image was captured using a fluorescence confocal microscope (Zeiss, Oberkochen, Germany).

Dual-luciferase reporter

Wild or mutated circ_0007411 or *PTPN12* 3'-UTR were synthesized into pGL3-luc plasmids containing luciferase reporter gene together with miR-548m (GenePharma, Shanghai, China). The plasmids were transiently transfected into hRECs using the Lipofectamine 3000 transfection system, and then the Dual Luciferase Assay System (Promega, Madison, WI, USA) was employed to test the firefly luciferase activity and Renilla activity.

Co-immunoprecipitation (Co-IP) and Western blotting

PTPN12 and SKP1 antibodies were added to extracts of lysed hRECs, respectively, then incubated for 12 h at 4 ℃. Sepharose beads coupled with Protein A were then added to the mixture and incubated for a further 4 h. The beads were washed twice with PBS and three times by washing buffer. After boiling with 50 μL of 1× sodium dodecyl sulfate (SDS) loading buffer for 10 min, the proteins were eluted then subjected to Western blotting assay as described in our previous work (18-20).

STZ-induced DR mouse model

Animal experiments were performed under a project license (No. 2019-398) granted by the Ethics Committee of Nanjing Medical University, in compliance with institutional guidelines for the humane treatment of animals, the Principles of Laboratory Animal Care (National Institutes of Health, Bethesda, MD, USA) (https://www.ncbi.nlm.nih.gov/books/NBK54050), and the ARVO Statement for the Use of Animals in Ophthalmic and Vision Research (https://www.arvo.org/About/policies/statement-for-the-use-of-animals-in-ophthalmic-and-vision-research/).

A total of 50 μg/g STZ was injected intraperitoneally into 8-week-old male C57BL/6 mice (purchased from Changzhou Cavens Laboratory Animals Co., Ltd.) for 5 days continuously. After an over 16.7 mmol/L blood glucose level (19), 80 μg/g ketamine was intraperitoneally injected together with 4 μg/g xylazine, and then the mice received an intravitreal injection of ~1.5 μL (1×10^{12} TU/mL) of AAV carrying mouse PTPN12 complementary DNA (cDNA) every 4 weeks. For shPTPN12 (5'-CACCGGACATACTG CCATTTGATCACGAATGATCAAATGGCAGTATGT CC-3'), the mice were administered an intravitreal injection (2 nmoL) every 2 weeks. The animals were grouped as: normal, STZ, STZ NC, STZ + OE-PTPN12, STZ + shPTPN12, with 5 mice in each group. After approximately 16 weeks, the retinal was recovered and investigated using Evans blue leakage and retinal trypsin digestion assays in our previous work (19). The eyeballs were enucleated and fixed with 4% paraformaldehyde for 24 h, and the retina and sclera were embedded in paraffin after dehydration. In hematoxylin and eosin (H&E) staining, 5-μm-thick sections were taken along the vertical meridian and were visualized using an Olympus BX-51 light microscope.

Statistical analysis

All *in vitro* experiments were repeated at least three times and all data were expressed as the average ± standard deviation (SD). *T*-test and one-way ANOVA were employed for comparisons between two groups or multiple groups in SPSS software (v 13.0). A P value of <0.05 was considered statistically significant.

Results

TTR-induced high level of circ_0007411 prevented the proliferation, migration, wound healing, and tube formation of hRECs in a high-glucose environment

In RNA-Seq and after TTR treatment, 78 differentially expressed circRNAs were identified, and circ_0007411 derived from PTPN12 was significantly upregulated (*Figure 1A*). qRT-PCR analysis indicated that in a high-glucose environment, the level of circ_0007411 was increased by the addition of TTR (*Figure 1B*). CCK-8 assay (*Table 2*) and EdU labelling (*Figure 1C,1D*) suggested the overexpression of circ_0007411 inhibited the proliferation of hRECs, whereas treatment with the two siRNAs promoted the proliferation. In FCM assay, the overexpression of circ_0007411 promoted the apoptosis ratio, whereas the siRNAs resulted in no significant differences (*Figure 1E,1F*). In Transwell assay, the migration of hRECs was repressed by overexpression of circ_0007411, but the siRNAs caused an increase (*Figure 1G*). Additionally, wound healing (*Figure 1H,1I*) and tube formation (*Figure 1J,1K*) were also suppressed by a high level of circ_0007411.

Circ_0007411 regulated the level of PTPN12 by targeting miR-548m

The NIH Circular RNA Interactome online service (https://circinteractome.nia.nih.gov/mirna_target_sites.html) and the TargetScanHuman online service (http://www.targetscan.org/vert_70/) were employed to screen the possible targets of circ_0007411 and the 3'-untranslation region (UTR) of *PTPN12*. The results suggested circ_0007411 [116–122] (*Figure 2A*) and the 3'-UTR of *PTPN12* mRNA [265–272] (*Figure 2B*) shared similar binding positions of miR-548m. To investigate whether miR-548m could bind with circ_0007411/*PTPN12* mRNA, the wild-type (WT) and mutant (MUT) sequences containing the candidate sites were transfected into hRECs, respectively, and the transient co-transfection with plasmids containing WT sites and miR-548m mimics showed decreased luciferase activities (*Figure 2A,2B*). In addition, the protein (*Figure 2C*) and mRNA (*Figure 2D*) levels of *PTPN12* were increased in hRECs after the overexpression of circ_0007411 but were suppressed by the knockdown of circ_0007411. In contrast, the level of miR-548m was repressed after the overexpression of circ_0007411 but was enhanced by the two siRNAs (*Figure 2E*).

Circ_0007411 might affect hRECs via the miR-548m/PTPN12/SKP1/EGFR pathway

To evaluate whether miR-548m could affect the hRECs in a high-glucose environment and to determine whether circ_0007411 could reverse these phenomena, miR-548m mimic, miR-548m inhibitor, and circ_0007411 overexpression plasmid (OECIRC) were co-transfected into hRECs. CCK-8 assay (*Table 3*), EdU labelling (*Figure 3A,3B*), Transwell (*Figure 3C*), wound healing (*Figure 3D,3E*), and tube formation (*Figure 3F,3G*) assays indicated miR-548m mimics could significantly promote the proliferation, migration, wound healing, and tube formation of hRECs, whereas the overexpression of circ_0007411 caused similar effects to the inhibitor of miR-548m and could partially rescue these processes. In addition, miR-548m mimics could significantly reduce the expression of *PTPN12*, although this phenomenon was rescued by the overexpression of circ_0007411 (*Figure 3H*). It has been previously reported that PTPN12 plays vital roles in tumor occurrence and development, cell apoptosis, cell cycle, and metabolism and may regulate the content of SKP1 and EGFR (12-14). In this study, the direct binding between PTPN12 and SKP1 was confirmed by co-IP assay (*Figure 3I*), and Western blotting analysis suggested the protein content of PTPN12, SKP1, and EGFR could be regulated by miR-548m mimic and rescued by circ_0007411 overexpression (*Figure 3J*). Interestingly, miR-548m mimic could not affect the expression of *SKP1* (*Figure 3K*), although it enhanced the expression of *EGFR* and was partially rescued by overexpression of circ_0007411 (*Figure 3L*).

The anti-retinal NV function of PTPN12 in DR mice

As circ_0007411 and miR-548m are not conserved in the mouse, in this work, only the overexpression and knockdown of *PTPN12* were performed in the DR mouse model to investigate the effects *in vivo*. Regarding *Figure 4A,4B*, the vascular leakage of retina in normal mice (10.1%±3.4%, 4/10 eyes) was not as severe as that in the STZ-treated DR mice (32.5%±4.7%, 4/10 eyes) and the STZ-treated NC mice (28.6%±1.9%, 4/10 eyes). The overexpression of PTPN12 (12.2%±1.3%, 4/10 eyes) could partially rescue the leakage ratio, whereas the knockdown of PTPN12 (44.6%±5.7%, 4/10 eyes) resulted in continuing deterioration.

Digested using trypsin, the average number of retinal acellular capillaries (10 fields) was significantly increased

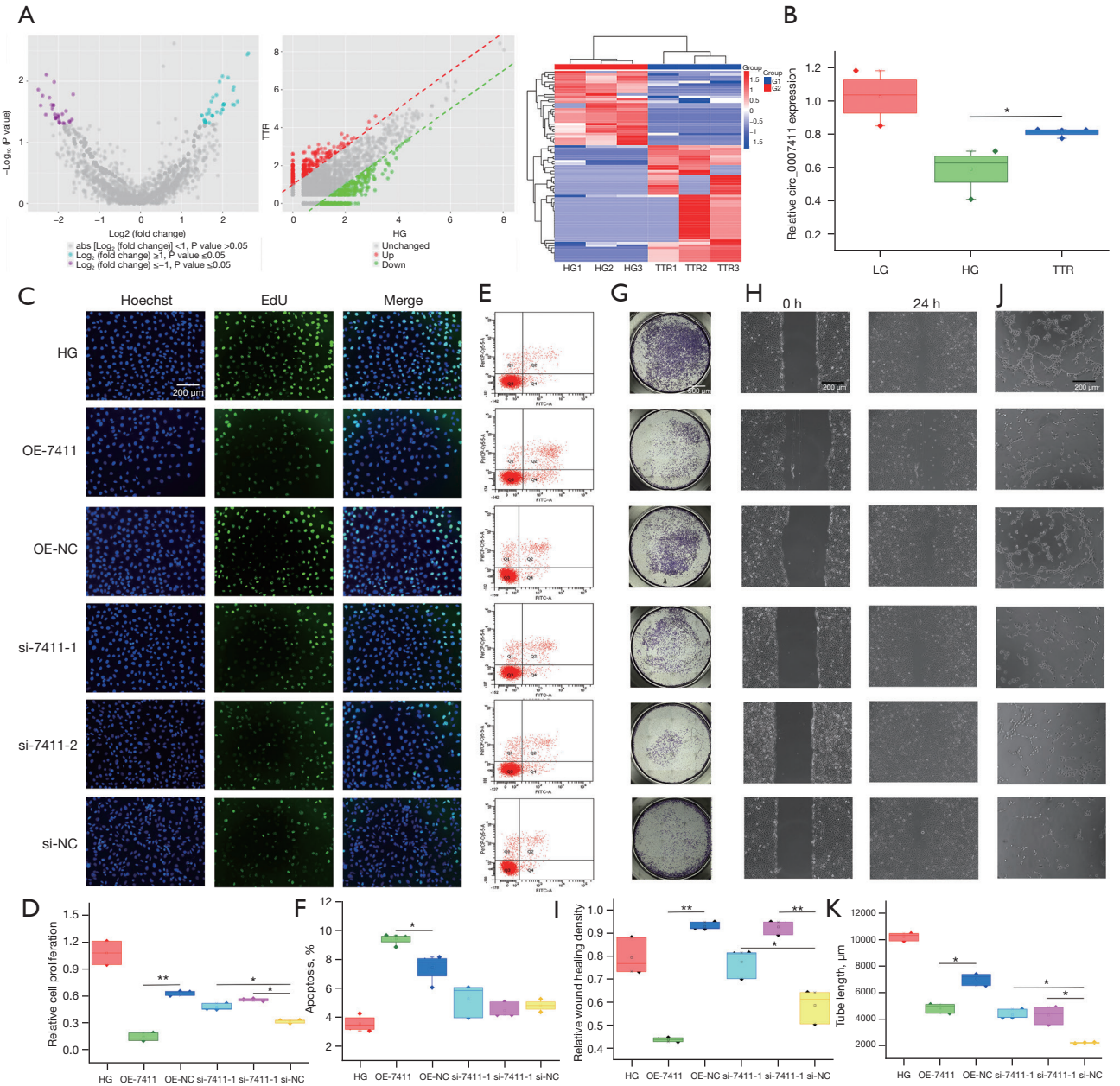

Figure 1 Effects of a TTR-induced high level of circ_0007411 on hRECs. (A) In RNA-Seq analysis, the volcano plot, scatter plot, and heatmap of inter-sample correlation showed the differential expression of circRNA between the HG and HG + TTR groups. (B) The circ_0007411 levels of hRECs under HG condition, in the presence or absence of TTR, and the circ_0007411 level in LG environment was used as a blank. (C,D) In the EdU assay, EdU was stained with Apollo 488 and the cell nucleus was stained with DAPI, and the proliferation ratio was calculated (scale bar =200 μm). (E,F) FCM was used to detect the proportion of hRECs in apoptosis. (G) Transwell assay was used to detect the migration of hRECs (crystal violet staining, scale bar =500 μm). (H,I) Wounding healing assay (scale bar =200 μm). (J,K) Tube formation assay (scale bar =200 μm). Error bars represent the mean ± SD of at least triplicate experiments. *, P<0.05; **, P<0.01. DAPI, 4',6-diamidino-2-phenylindole; EdU, 5-ethynyl-2'-deoxyuridine; FCM, flow cytometry; LG, low glucose; HG, high glucose; hRECs, human retinal microvascular endothelial cells; NC, negative control; OE; overexpression; RNA-Seq, RNA sequencing; SD, standard deviation; TTR, transthyretin.

Table 2 The index of hRECs affected by circ_0007411 under high glucose conditions

Groups	24 h		48 h		72 h	
	OD_{450nm}, mean ± SD	P value	OD_{450nm}, mean ± SD	P value	OD_{450nm}, mean ± SD	P value
HG	1.947±0.223		2.985±0.302		3.655±0.344	
OE-7411	1.235±0.083	OE-7411 *vs.* OE-NC, 0.086	2.107±0.124	OE-7411 *vs.* OE-NC, 0.030	2.860±0.130	OE-7411 *vs.* OE-NC, 0.042
OE-NC	1.458±0.088		2.536±0.188		3.295±0.121	
si-7411-1	1.424±0.074	si-7411-1 *vs.* si-NC, 0.715; si-7411-2 *vs.* si-NC, 0.278	2.617±0.156	si-7411-1 *vs.* si-NC, 0.042; si-7411-2 *vs.* si-NC, 0.028	3.331±0.160	si-7411-1 *vs.* si-NC, 0.033; si-7411-2 *vs.* si-NC, 0.040
si-7411-2	1.502±0.093		2.589±0.123		3.264±0.122	
si-NC	1.385±0.088		2.190±0.070		2.793±0.147	

HG, high glucose; OE, overexpression; NC, negative control; hRECs, human retinal microvascular endothelial cells; OD, optical density; SD, standard deviation.

from 3±1 of normal mice (4/10 eyes) to 10±2 of STZ-treated DR mice (4/10 eyes) and 11±2 of STZ-treated NC mice (4/10 eyes) but was partially rescued together with the overexpression of PTPN12 (11±2, 4/10 eyes), whereas the knockdown of PTPN12 resulted in continuing deterioration (15±2, 4/10 eyes) (*Figure 4C*,*4D*). In addition, as shown in *Figure 4C*,*4E*, the hRECs:pericytes ratio (3.2±0.3, 4/10 eyes) was significantly increased in STZ-treated DR mice (7.1±0.8, 4/10 eyes) and STZ-treated NC mice (7.9±1.0, 4/10 eyes), which was associated with the loss of pericytes. The overexpression of PTPN12 partially reversed the loss of pericytes (5.7±0.7, 4/10 eyes), whereas the knockdown of PTPN12 resulted in continuing deterioration (10.2±1.1, 4/10 eyes). Furthermore, the detachment of the retina and choroid in STZ-treated DR mice was partially rescued by overexpression of PTPN12 but was much more severe after the knockdown of PTPN12 (*Figure 4F*).

Discussion

Diabetes has recently emerged as a global health risk, and DR is one of the most severe complications (2,3). TTR is a 55-kDa homo-tetramer protein which is normally known as the carrier protein of thyroxine (T4) and retinol in plasma and cerebrospinal fluid. TTR has been proven to have anti-retinal NV function in DR *in vitro* and *in vivo* through the TTR/PABPC1/lncRNA MEG3/miR-223-3p/FBXW7 and TTR/hnRNPA2B1/STAT4/miR-223-3p/FBXW7 signaling axis (18-20). CircRNAs have been found to play important roles in the mechanism of different diseases, including DR (7-10).

In this work, to screen potential circRNAs that may have been regulated by TTR in hypoglycemia, RNA-Seq was employed. Circ_0007411 from *PTPN12* was seen to be promoted by TTR in a high-glucose environment and the mechanism is thought to be associated with the formation of the TTR-hnRNPA2B1 complex, because hnRNPA2B1 has been shown to have mRNA editing activity (20). The overexpression of circ_0007411 could significantly repress the proliferation, migration, wound healing, and tube formation of hRECs in a high-glucose environment, and could promote the proportion of cells in undergoing apoptosis. Another interesting result was that the expression of *PTPN12*, the parent gene of circ_0007411, was enhanced at both the mRNA and protein levels. *PTPN12* has been reported to exert antitumor effects by regulating EGFR (15-17), and SKP1 has been reported to participate in cancer development, and is predicted to regulate EGFR (25,26). However, the details of the mechanism are still unclear.

Predicted using NIH Circular RNA Interactome (https://circinteractome.nia.nih.gov/mirna_target_sites.html) and TargetScanHuman (http://www.targetscan.org/vert_70/), miR-548m was the binding target of circ_0007411 and the 3'-UTR of *PTPN12* mRNA, and the direct interaction was confirmed by dual-luciferase reporter assay. In the qRT-PCR assay, the overexpression of circ_0007411 significantly promoted the expression of *PTPN12*, whereas miR-548m mimics repressed it, and overexpression of circ_0007411 rescued the effects of miR-548m. In addition, in the physiological assays, the proliferation, migration, wound healing, and tube formation progressions were significantly promoted with miR-548m mimics, while these phenomena could be partially rescued by overexpressed circ_0007411. These results suggested that a high level of circ_0007411 could promote the expression of *PTPN12* via repression of the miR-548m. Although miR-538m has been reported

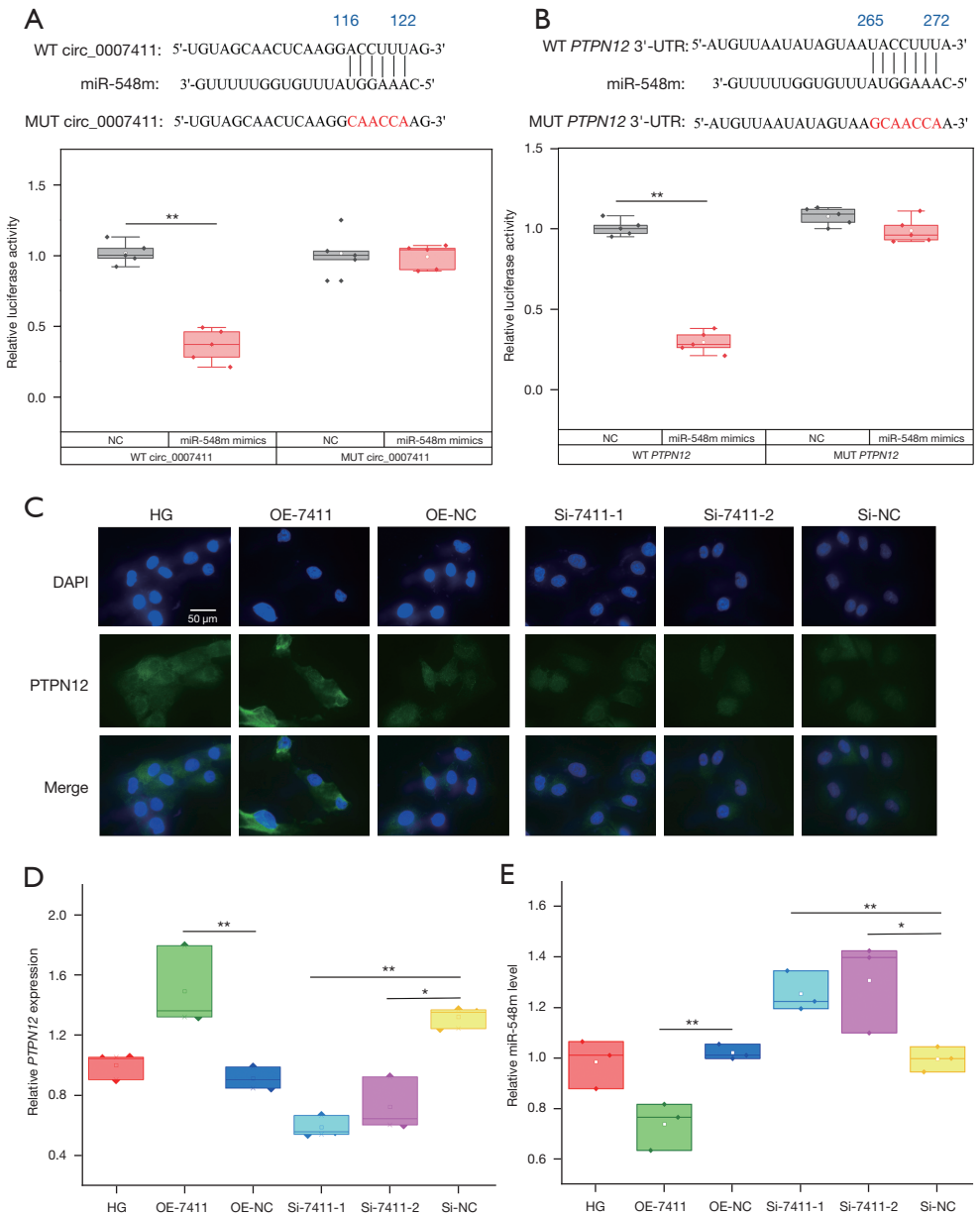

Figure 2 Circ_0007411 regulated the level of PTPN12 and miR-548m. (A) Binding sites of circ_0007411 and miR-548m. The luciferase reporter with the WT or MUT sequences of circ_0007411 transfected together with miR-548m mimics or negative controls. (B) Binding sites of the 3'-UTR of *PTPN12* mRNA and miR-548m. The luciferase reporter with the WT or MUT 3'-UTR of *PTPN12* mRNA sequences were transfected together with miR-548m mimics or negative controls. (C) The nucleus was stained with DAPI, whereas the PTPN12 in hRECs was recognized by mouse anti-human PTPN12 antibody and Alexa Fluor 488-labeled donkey anti-mouse IgG antibody (scale bar =50 μm). The expression of *PTPN12* (D) and miR-548m (E) was affected by circ_0007411. Error bars represent the mean ± SD of at least triplicate experiments. *, P<0.05; **, P<0.01. WT, wild type; MUT, mutant; UTR, untranslated region; DAPI, 4',6-diamidino-2-phenylindole; PTPN12, protein tyrosine phosphatase nonreceptor type 12; hRECs, human retinal microvascular endothelial cells; SD, standard deviation; NC, negative control; OE, overexpression.

Table 3 The index of hRECs affected by mir-548m and circ_0007411 under high glucose conditions

Groups	24 h		48 h		72 h	
	OD_{450nm}, mean ± SD	P value	OD_{450nm}, mean ± SD	P value	OD_{450nm}, mean ± SD	P value
HG	2.021±0.176		3.028±0.272		3.812±0.197	
Mi-NC	1.833±0.140	Mimic *vs.* mi-NC, 0.014; mimic *vs.* mimic + 7411, 0.039	2.122±0.083	Mimic *vs.* mi-NC, 0.004; mimic *vs.* mimic + 7411, 0.009	2.993±0.103	Mimic *vs.* mi-NC, 0.008; mimic *vs.* mimic + 7411, 0.005
Mimic	2.437±0.109		2.730±0.101		3.455±0.107	
Mimic + 7411	2.107±0.074		2.187±0.112		2.915±0.111	
In-NC	1.554±0.082	In-NC *vs.* inhibitor, 0.108	2.776±0.084	In-NC *vs.* inhibitor, 0.031	3.032±0.121	In-NC *vs.* inhibitor, 0.025
Inhibitor	1.389±0.060		2.333±0.150		2.560±0.110	

HG, high glucose; hRECs, human retinal microvascular endothelial cells; OD, optical density; mi-NC, mimic-negative control; in-NC, inhibitor-negative control; SD, standard deviation.

to suppress the migration and invasion of breast cancer cells (27), it may perform the opposite function in hRECs. We speculated there was a potential interaction between PTPN12 and SKP1 and confirmed the direct binding of PTPN12 and SKP1 in a co-IP assay. Moreover, in a Western blotting assay, miR-548m mimics could regulate the protein levels of PTPN12, SKP1 and EGFR, while the overexpression of circ_0007411 could rescue it. Further, in qRT-PCR assay, miR-548m could only affect the expression of *EGFR* but not *SKP1*. These results suggested SKP1 is a direct downstream molecule of PTPN12, and that EGFR is a potential downstream factor of the PTPN12-SKP1 complex, although further investigation is required to determine the details. Additionally, as inflammation has been considered as a central role player in DR, and in our previous work, the antagonistic mechanism of miR-1243 against RELB/circ_0008590 in NF-κB non-classic pathway was proved to repress the NV progression of DR (28); in this work, we tried to investigate the relationship between circ_0007411 and classic inflammation signaling pathways, however, the overexpression and knockdown of circ_0007411 could not affect the factors in NF-κB, TLR and Jak/Stat pathways.

As circ_0007411 and miR-548m are not conserved in mice, in this work, the function of *PTPN12* was investigated by establishing an STZ-induced model of DR in C57BL/6 mice. The *in vivo* results were in good accordance with the *in vitro* results in hRECs, and the high expression of *PTPN12* significantly reduced the procession of DR (29), while the retinal vascular leakage, acellular capillary, loss of pericyte, and the detachment of retina and choroid were all significantly rescued.

Recently, intraocular injection of anti-VEGF antibodies has been considered as the most frequently used clinical therapy for DR, and circ_0007411 should be of great potential as a concomitant candidate. The results of this work suggested that circ_0007411 could relieve the clinical progression of DR through a different pathway together with anti-VEGF therapy. However, owing to the stable and tight ocular barriers (30), how to deliver circ_0007411 into the eye and to keep a stable level in retinal are still critical challenges; more delivering and sustained releasing protocols should be investigated.

In summary, this was the first study to investigate the TTR-induced high level of circ_0007411 and its downstream mechanism. The identified interaction between circ_0007411, *PTPN12* mRNA, and miR-548m, and the direct binding of PTPN12 and SKP1 suggested that circ_0007411 plays a significant role in the anti-angiogenesis process via the miR-548m/PTPN12/SKP1/EGFR signaling pathway (*Figure 5*).

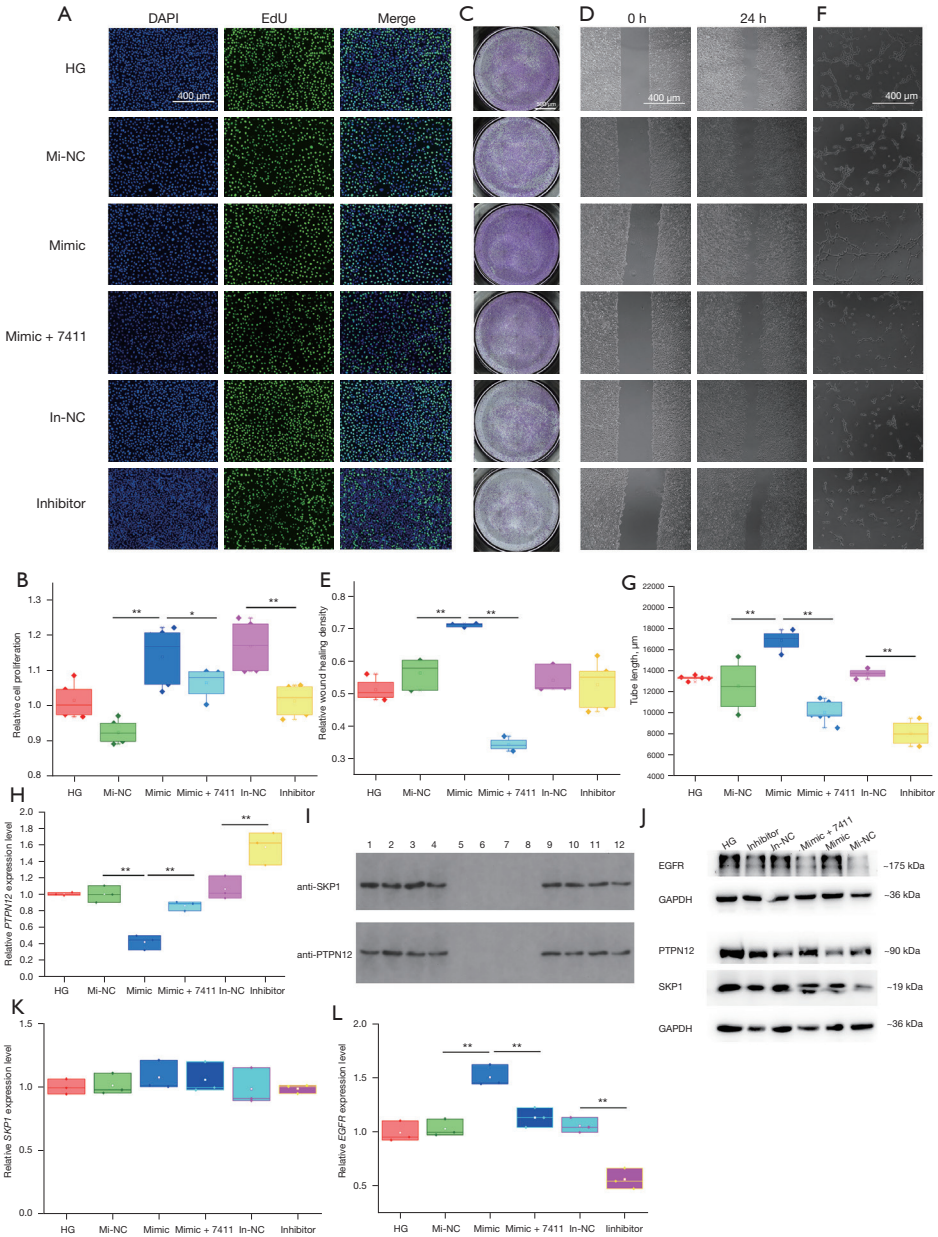

Figure 3 Overexpression of circ_0007411 partially rescued the effects of miR-548m mimics on hRECs. (A,B) EdU assay. EdU was stained with Apollo 488 and the nucleus was stained with DAPI, and the proliferation ratio was calculated (scale bar =400 μm). (C) Transwell assay was used to detect the migration of hRECs (crystal violet staining, scale bar =500 μm). (D,E) Wound healing assay (scale bar =400 μm). (F,G) Tube formation assay (scale bar =400 μm). (H) miR-548m mimics altered the expression of *PTPN12*. (I) Co-IP of PTPN12 and SKP1: lanes 1–4 were four parallel inputs containing the whole protein of the lysed hRECs; lanes 5–8 were four parallel blank controls; and lanes 9–12 were parallel samples to lanes 1–4 captured by anti-SKP1 or anti-PTPN12 antibodies. The membranes were incubated with anti-PTPN12 or anti-SKP1 antibodies, respectively. (J) The miR-548m mimics altered the levels of downstream proteins. (K) Effects of miR-548m mimics on the expression of *SKP1*. (L) Effects of miR-548m mimics on the expression of *EGFR*. Error bars represent the mean ± SD of at least triplicate experiments. *, P<0.05; **, P<0.01. Co-IP, co-immunoprecipitation; DAPI, 4',6-diamidino-2-phenylindole; EdU, 5-Ethynyl-2'-deoxyuridine; EGFR, epidermal growth factor receptor; GAPDH, glyceraldehyde 3-phosphate dehydrogenase; HG, high glucose; hRECs, human retinal microvascular endothelial cells; NC, negative control; mi-NC, mimic-negative control; in-NC, inhibitor-negative control; PTPN12, protein tyrosine phosphatase nonreceptor type 12; SD, standard deviation; SKP1, S-phase kinase associated protein 1.

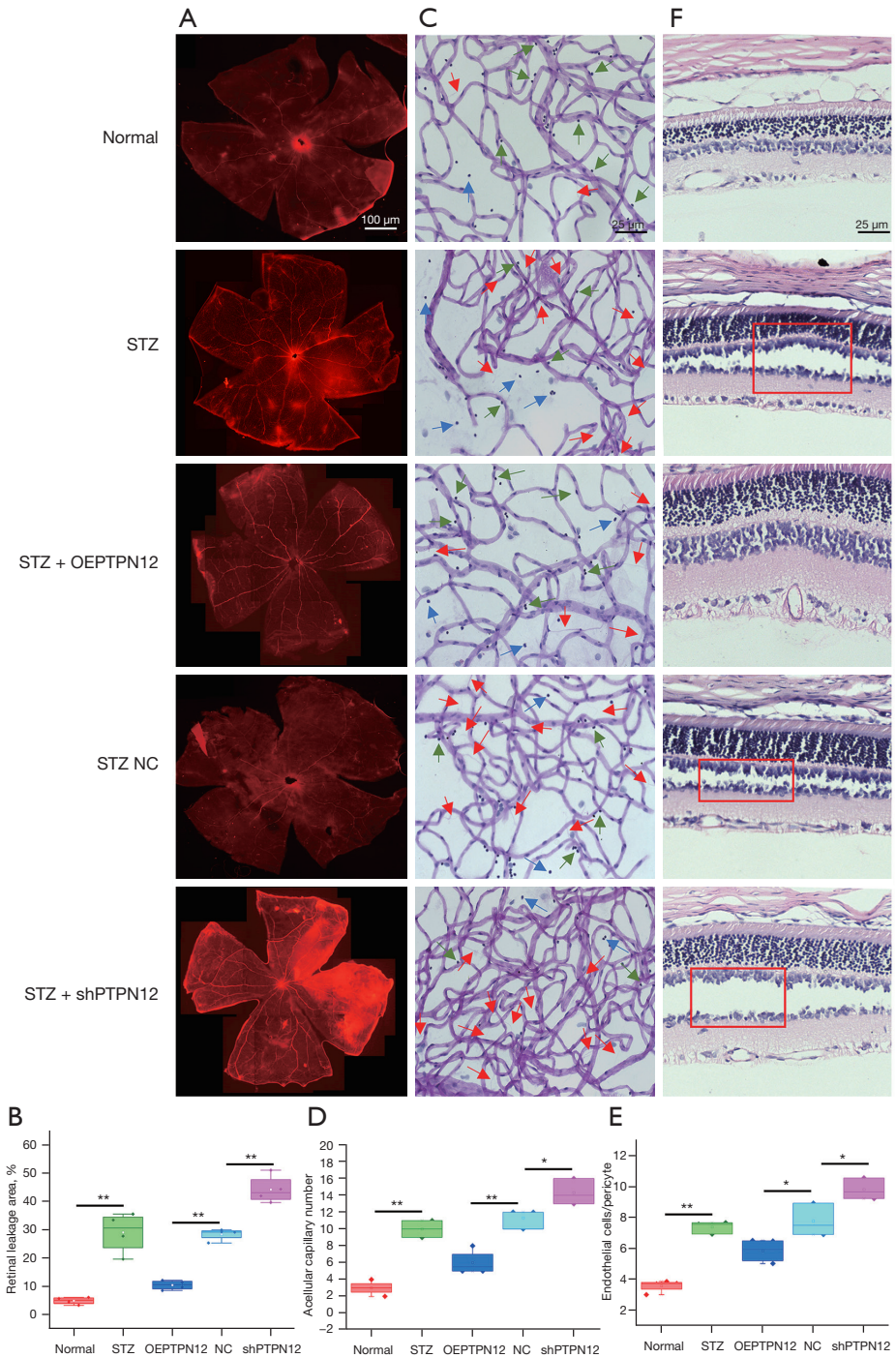

Figure 4 The effects of PTPN12 in STZ-induced DR mice. (A,B) Stained with Evans blue, the retinal vascular leakage was detected (scale bar =100 μm). After trypsin digestion of the retina (C) (stained with periodic acid-Schiff, scale bar =25 μm), the number of acellular capillaries (D) and the hRECs:pericytes ratio (E) were counted (red arrows, the acellular capillaries; green arrows, the maintained pericytes; blue arrows, the lost pericytes). (F) In prepared 5-μm sections of dehydrated retina and sclera, the detachment between retina and choroid was marked with a red rectangle (H&E staining, scale bar =25 μm). Error bars represent the mean ± SD of at least triplicate experiments. *, P<0.05; **, P<0.01. DR, diabetic retinopathy; hRECs, human retinal microvascular endothelial cells; H&E, hematoxylin and eosin; NC, negative control; PTPN12, protein tyrosine phosphatase nonreceptor type 12; OE, overexpression; SD, standard deviation; STZ, streptozotocin.

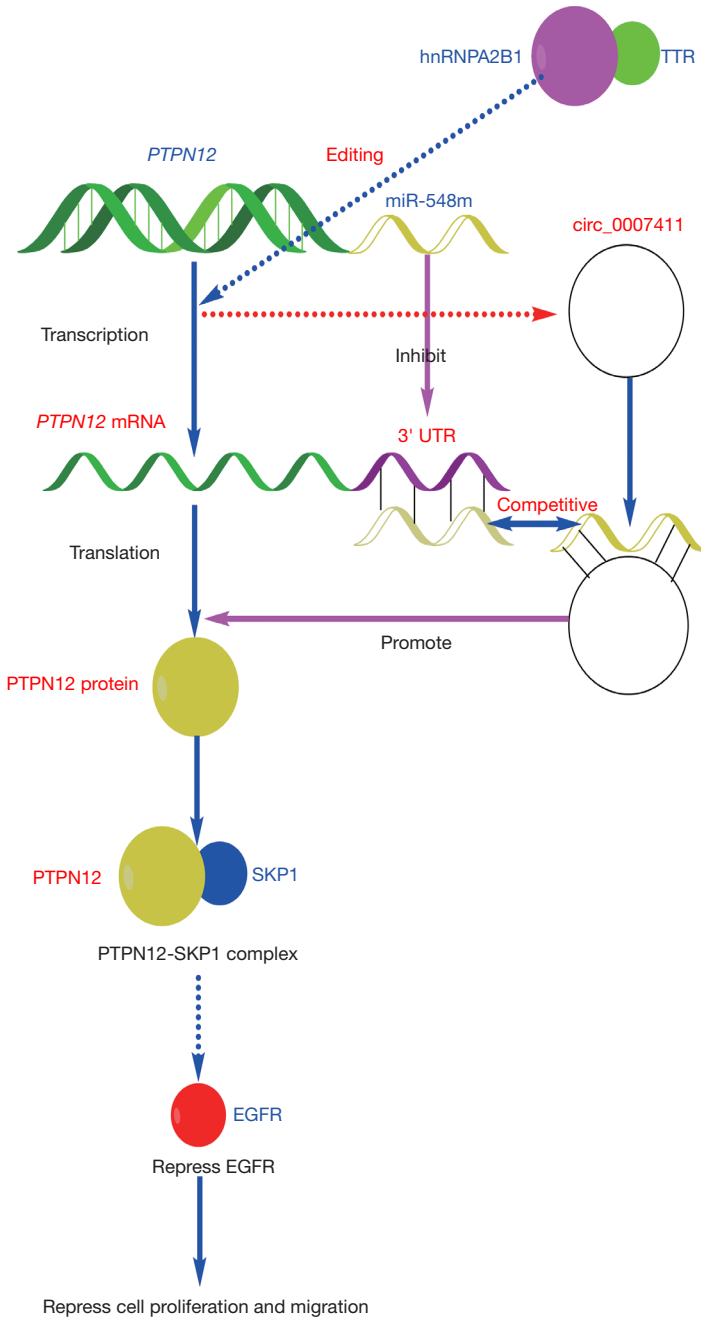

Figure 5 The potential mechanism of this study. In a high-glucose environment, the TTR-induced high level of circ_0007411 could promote the expression of *PTPN12* by binding with miR-548m. The increased PTPN12 helped to form the PTPN12-SKP1 complex and finally reduced the protein content of EGFR, leading to the suppression of cell proliferation and migration. EGFR, epidermal growth factor receptor; PTPN12, protein tyrosine phosphatase nonreceptor type 12; SKP1, S-phase kinase associated protein 1; TTR, transthyretin; UTR, untranslated region.

Acknowledgments

Funding: This work was supported by the National Natural Science Foundation of China (No. 81970819), China Postdoctoral Science Foundation (No. 2020M671541), and Youth Medical Talent Project of Jiangsu Province (No. QNRC2016182).

Footnote

Reporting Checklist: The authors have completed the ARRIVE reporting checklist. Available at https://atm.amegroups.com/article/view/10.21037/atm-22-1276/rc

Data Sharing Statement: Available at https://atm.amegroups.com/article/view/10.21037/atm-22-1276/dss

Conflicts of Interest: All authors have completed the ICMJE uniform disclosure form (available at https://atm.amegroups.com/article/view/10.21037/atm-22-1276/coif). The authors have no conflicts of interest to declare.

Ethical Statement: The authors are accountable for all aspects of the work in ensuring that questions related to the accuracy or integrity of any part of the work are appropriately investigated and resolved. Animal experiments were performed under a project license (No. 2019-398) granted by the Ethics Committee of Nanjing Medical University, in compliance with institutional guidelines for the humane treatment of animals, the Principles of Laboratory Animal Care (National Institutes of Health, Bethesda, MD, USA), and the ARVO Statement for the Use of Animals in Ophthalmic and Vision Research.

References

1. Wong TY, Sabanayagam C. Strategies to Tackle the Global Burden of Diabetic Retinopathy: From Epidemiology to Artificial Intelligence. Ophthalmologica 2020;243:9-20.
2. Amoaku WM, Ghanchi F, Bailey C, et al. Diabetic retinopathy and diabetic macular oedema pathways and management: UK Consensus Working Group. Eye (Lond) 2020;34:1-51.
3. Ting DS, Cheung GC, Wong TY. Diabetic retinopathy: global prevalence, major risk factors, screening practices and public health challenges: a review. Clin Exp Ophthalmol 2016;44:260-77.
4. Klein R, Lee KE, Gangnon RE, et al. The 25-year incidence of visual impairment in type 1 diabetes mellitus the wisconsin epidemiologic study of diabetic retinopathy. Ophthalmology 2010;117:63-70.
5. Capitão M, Soares R. Angiogenesis and Inflammation Crosstalk in Diabetic Retinopathy. J Cell Biochem 2016;117:2443-53.
6. Lu L, Jiang Y, Jaganathan R, et al. Current Advances in Pharmacotherapy and Technology for Diabetic Retinopathy: A Systematic Review. J Ophthalmol 2018;2018:1694187.
7. Zhou HR, Kuang HY. Circular RNAs: Novel target of diabetic retinopathy. Rev Endocr Metab Disord 2021;22:205-16.
8. Chen LL. The expanding regulatory mechanisms and cellular functions of circular RNAs. Nat Rev Mol Cell Biol 2020;21:475-90.
9. Guo N, Liu XF, Pant OP, et al. Circular RNAs: Novel Promising Biomarkers in Ocular Diseases. Int J Med Sci 2019;16:513-8.
10. He M, Zhou R, Liu S, et al. Circular RNAs: Potential Star Molecules Involved in Diabetic Retinopathy. Curr Eye Res 2021;46:277-83.
11. Li D, Liu C, Sun YN, et al. Targeting choroidal vascular dysfunction via inhibition of circRNA-FoxO1 for prevention and management of myopic pathology. Mol Ther 2021;29:2268-80.
12. Shan K, Liu C, Liu BH, et al. Circular Noncoding RNA HIPK3 Mediates Retinal Vascular Dysfunction in Diabetes Mellitus. Circulation 2017;136:1629-42.
13. Zou J, Liu KC, Wang WP, et al. Circular RNA COL1A2 promotes angiogenesis via regulating miR-29b/VEGF axis in diabetic retinopathy. Life Sci 2020;256:117888.
14. Lee C, Rhee I. Important roles of protein tyrosine phosphatase PTPN12 in tumor progression. Pharmacol Res 2019;144:73-8.
15. Li H, Yang F, Liu C, et al. Crystal Structure and Substrate Specificity of PTPN12. Cell Rep 2016;15:1345-58.
16. de Voer RM, Hahn MM, Weren RD, et al. Identification

of Novel Candidate Genes for Early-Onset Colorectal Cancer Susceptibility. PLoS Genet 2016;12:e1005880.
17. Lin Q, Wang H, Lin X, et al. PTPN12 Affects Nasopharyngeal Carcinoma Cell Proliferation and Migration Through Regulating EGFR. Cancer Biother Radiopharm 2018;33:60-4.
18. Shao J, Fan G, Yin X, et al. A novel transthyretin/STAT4/miR-223-3p/FBXW7 signaling pathway affects neovascularization in diabetic retinopathy. Mol Cell Endocrinol 2019;498:110541.
19. Fan G, Gu Y, Zhang J, et al. Transthyretin Upregulates Long Non-Coding RNA MEG3 by Affecting PABPC1 in Diabetic Retinopathy. Int J Mol Sci 2019;20:6313.
20. Gu Y, Hu D, Xin Y, et al. Transthyretin affects the proliferation and migration of human retinal microvascular endothelial cells in hyperglycemia via hnRNPA2B1. Biochem Biophys Res Commun 2021;557:280-7.
21. Shao J, Zhang Y, Fan G, et al. Transcriptome analysis identified a novel 3-LncRNA regulatory network of transthyretin attenuating glucose induced hRECs dysfunction in diabetic retinopathy. BMC Med Genomics 2019;12:134.
22. Dai M, Thompson RC, Maher C, et al. NGSQC: cross-platform quality analysis pipeline for deep sequencing data. BMC Genomics 2010;11 Suppl 4:S7.
23. Kim D, Pertea G, Trapnell C, et al. TopHat2: accurate alignment of transcriptomes in the presence of insertions, deletions and gene fusions. Genome Biol 2013;14:R36.
24. Zhang XO, Wang HB, Zhang Y, et al. Complementary sequence-mediated exon circularization. Cell 2014;159:134-47.
25. Mertins P, Mani DR, Ruggles KV, et al. Proteogenomics connects somatic mutations to signalling in breast cancer. Nature 2016;534:55-62.
26. Tian C, Lang T, Qiu J, et al. SKP1 promotes YAP-mediated colorectal cancer stemness via suppressing RASSF1. Cancer Cell Int 2020;20:579.
27. Wm Nor WMFSB, Chung I, Said NABM. MicroRNA-548m Suppresses Cell Migration and Invasion by Targeting Aryl Hydrocarbon Receptor in Breast Cancer Cells. Oncol Res 2021;28:615-29.
28. Shao J, Cai J, Yao Y, et al. Hyperglycemia-induced increasing of RELB/circ_0008590 in NF-κB pathway is repressed by miR-1243 in human retinal microvascular endothelial cells. Ann Transl Med 2021;9:1624.
29. Kur J, Newman EA, Chan-Ling T. Cellular and physiological mechanisms underlying blood flow regulation in the retina and choroid in health and disease. Prog Retin Eye Res 2012;31:377-406.
30. Lee J, Pelis RM. Drug Transport by the Blood-Aqueous Humor Barrier of the Eye. Drug Metab Dispos 2016;44:1675-81.

(English Language Editor: B. Draper)

Cite this article as: Hu D, Tian Y, Ye L, Xin Y, Shao J. Transthyretin-induced increase in circ_0007411 represses neovascularization of human retinal microvascular endothelial cells in hyperglycemia via the miR-548m/PTPN12/SKP1/EGFR pathway. Ann Transl Med 2022;10(10):556. doi: 10.21037/atm-22-1276

